

Thermal Gradient Solid State Forming of Polypropylene

J. C. W. Lo, D. M. Shinozaki

Department of Mechanical and Materials Engineering, The University of Western Ontario, London, Canada N6A 5B9

Received 4 September 2006; accepted 13 June 2007

DOI 10.1002/app.26950

Published online 27 December 2007 in Wiley InterScience (www.interscience.wiley.com).

ABSTRACT: The near surface region of polypropylene was hardened in a forming process, which involved a large shear strain in a strong thermal gradient. The optimal processing conditions were estimated by modeling the temperature distribution in the deformation zone. Microindentation testing was used to characterize the corresponding depth-dependent mechanical properties. The

mechanical gradient, which developed after forming, was consistent with the observed variation in microstructure. © 2007 Wiley Periodicals, Inc. *J Appl Polym Sci* 108: 148–158, 2008

Key words: thermal gradient; surface hardening; polypropylene; microindentation

INTRODUCTION

The development of molecular and crystallite orientation in polymers results in increasing anisotropy of mechanical properties, with enhanced modulus and tensile strength in the orientation direction.^{1,2} It is of some interest to develop simple processing methods that exploit orientation in polymers to produce local hardening in near surface regions.

It is well known that preferred orientation of lamellae can be produced in polypropylene by hot drawing in the solid state.^{3,4} At elevated temperatures, the modulus and tensile strength increase with the increase in tensile strain.⁴ The flow stress of the material is inversely related to the temperature: higher temperatures result in lower flow stresses. This general principle has been suggested as a solid-state forming process to produce complex profiles in metal forging.⁵ In metals, it is therefore possible to produce graded properties by inducing a thermal gradient in the solid, and concurrently imposing shear strain on the hot surface. With increasing distance from the heated surface, the temperature decreases and the flow stress increases. For a uniform-applied stress, the plastic strain rate decreases as the flow stress increases. Hence by controlling the temperature field, a strain gradient can be imposed on the specimen. In polymers, the fabrication of graded mechanical properties is less well understood.

This work examines the development of orientation in near surface regions of polypropylene using

large strain shear of the surface in the solid state. It is known that large strains produce microstructural orientation in polymers, and that mechanical properties are influenced by the lamellar and molecular orientation generated by plastic strains in the solid state. The article examines the phenomenology of the process rather than the detailed local physics. The thermomechanical process involves a large strain deformation of a highly localized volume of the material, within which the strain rate and strain gradients are large. There is therefore a sharp gradient in the microstructural processes, which occur during forming, and it is not possible to obtain experimental measurements of the spatial distribution of the molecular processes occurring during processing. The physical processes postulated are inferred from the correlation of the experimental observations with well-documented observations in hot drawing of polypropylene.

MATERIALS AND METHODS

Samples of compression-molded commercial sheet (thickness = 13 mm) polypropylene were cut and machined into rectangular pieces (152 × 13 × 28 mm³). A schematic diagram of the forming die is shown in Figure 1 (not to scale). The height of the specimen (*y*-direction) was 28 mm. The sample (A) was driven by the ram (Sintech) over an electrically heated plate (B) and past the lip of the die (D), where the large strain localized to the bottom surface was generated. The temperature of the plate (B) was controlled to 160°C while the opposite face (C) was at room temperature. The tapered constriction at (C) compressed the rectangular specimen tightly against the hot top surface (B) as the specimen is driven forward in the $-x$ direction.

Correspondence to: D. M. Shinozaki (shinozaki@uwo.ca).
Contract grant sponsor: NSERC Discovery.

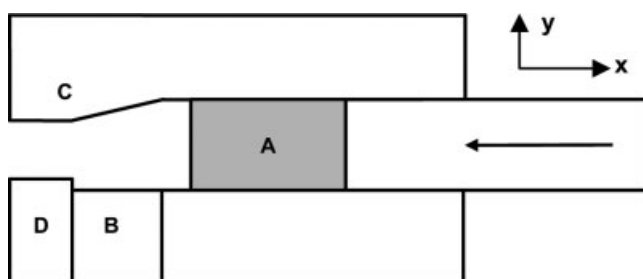


Figure 1 Schematic diagram of forming die (not to scale): (A) specimen; (B) heated plate; (C) tapered restriction; (D) forming lip.

The geometry of the forming process ensured that the heated side of the specimen was forced across the sharp shoulder (lip) at D. The height of the lip is ~ 0.2 mm. A temperature-gradient dT/dy was formed across the specimen. The shear at the die lip was imposed within this temperature gradient, and a strain gradient developed in the sample in the y direction.

The specimen was forced through the die by a steel ram, which was, in turn, driven by a Sintech tension/compression tester at a constant velocity. This crosshead speed was adjusted over a range from 0.20 to 100 mm/min. Adjustment of the processing speed allowed for the optimization of the ram velocity to obtain the desired temperature gradient. The deformed sample was cooled to room temperature before removing it from the die. The temperature of the hot die was controlled at $(160 \pm 1)^\circ\text{C}$, which is just below the nominal melting temperature of polypropylene (163°C).

The variation of the microstructure from point to point was examined using thin sections cut with a microtome and transmitted light optical microscopy using crossed polars. In addition, the degree of crystal orientation in the polypropylene was measured by two-dimensional wide angle X-ray diffraction patterns (WAXP). These were recorded in transmission using unfiltered radiation from a Cu target running at 40 kV and 20 mA. One-dimensional wide angle X-ray diffractometer scans were made using Ni-filtered Cu $K\alpha$ radiation at a scan rate of $0.1^\circ/\text{min}$. (20).

Dynamic mechanical tests were run as a function of temperature on samples cut parallel to the deformed surface (thickness = 1.7 mm). A Polymer Laboratories DMTA was used in bending mode (2 Hz), the orientation of the specimen chosen to measure the longitudinal modulus (x -direction). The thermal properties were measured using differential scanning calorimetry (DSC) in heating mode at a temperature scanning rate of $10^\circ\text{C}/\text{min}$. These specimens (approximate thickness = 0.1 mm) were cut from different regions of the formed specimen to measure melting behavior of the crystalline fraction of the polypropylene.

The variation of local mechanical properties was measured using microindentation. This instrument consists of a small diameter ($80 \mu\text{m}$) flat cylindrical punch driven by a computer-controlled piezoelectric actuator. The instrumentation allowed for the measurement of load as a function of indenter displacement.

RESULTS AND DISCUSSION

The forming process involved the development of a strain gradient in a moving temperature field. The basic principle involved setting up a temperature gradient in the surface. The mechanical properties of polypropylene vary with temperature, and a strain gradient was produced within the temperature field. The temperature field in the process region depended on the applied temperature, the heat flow within the zone and the velocity of the specimen across the heat source. Given the design of the initial specimen and die, the range of appropriate velocities of the ram needed to be determined. An initial step in this was the estimation of the temperature field in the specimen during forming.

Thermal gradients

The use of thermocouples to measure temperatures within the sample volume was problematical because of the relatively high thermal conductivity of the probes. The small heat capacity and poor thermal conductivity of the polypropylene meant local temperatures would be distorted by the heat flow along the probe wires. It was thought that a numerical calculation would provide a more accurate estimation of the temperature field, since the problem was well defined and the material thermal properties were known.

The work generated from the deformation of the material can increase the temperature of the workpiece. This can be estimated from the maximum expected plastic strain in the processing zone in the workpiece and considered in terms of heat generated and lost. The temperature rises as a result of the heat generated by the plastic work done on the specimen. The area under the stress-strain curve for the material is a measure of the work done per unit volume of the deforming material. Published experimental measurements on macroscopic sheets of ductile polymers⁶ show that the temperatures rise $\sim 15^\circ\text{C}$ above the ambient temperature (room temperature) for tensile drawing. For deformation at elevated temperatures, as in this study, the work done, and the resulting temperature rise, is reduced to $\sim 1/3$ of that estimated for the room temperature deformation since at elevated temperatures the stresses are reduced (the exact reduction depends on

the drawing temperature). Using a measured tensile stress–strain curve for polypropylene at elevated temperature, an estimate indicates that there could be a maximum adiabatic temperature rise of $\sim 5^\circ\text{C}$ above the ambient temperature.

The increase in temperature from the deformation work done in the region near the contact with the die will be reduced by conduction and convection. The relatively small size of the deforming volume will result in a rapid heat transfer to the surrounding material and air. This size effect has been ascribed to the increase in surface to volume ratio as the deforming volume becomes smaller, for plastically deforming polypropylene.⁷

In the present experiments, a more accurate estimate is complicated by the sharp gradients in temperature and strain imposed by the forming process. Since the temperature rise is affected by the rate of heat transfer away from the deforming zone, the local strain rate will affect the local temperature. It should be noted that the coefficient of thermal conductivity depends on the crystallinity, and the local orientation of the lamellae since anisotropic polymer crystals have strong anisotropy in conductivity. The complexity of the time and spatial dependences of the evolving microstructure during forming precludes an accurate estimate of the local temperature rise which develops. An approximation based on the earlier discussion would suggest a deformation-induced temperature rise of the order of $1\text{--}3^\circ\text{C}$ at most, which is ignored in the present modeling.

In terms of practical processing of thermoplastics, the strain field in the material in the region (B) was of interest. The temperature field in the region (B) in Figure 1 during forming was therefore calculated. The problem is a dynamic one since the material is pushed through the die and traverses the heated plate (B). Although the results are shown here for a two-dimensional cut, the calculation was made in three dimensions, accounting for heat loss in the lateral directions. The three-dimensional temperature field was first calculated to obtain some idea of the spatial extent of the processing zone in the near surface region of the material. An explicit finite difference method was used to approximate the analytical solution of the well-known constant density heat equation:

$$\nabla^2 T = \frac{1}{\alpha} \frac{\partial T}{\partial t} \quad (1)$$

where T is temperature and t is time, and it was assumed that there was no internal heat generation (the work generated in the inelastic deformation was ignored). The thermal diffusivity was

$$\alpha = \frac{k}{\rho C_p} \quad (2)$$

where $k = 0.17 \text{ W/mK}$ was the thermal conductivity for polypropylene, $\rho = 910 \text{ kg/m}^3$ was the density, and $C_p = 2140 \text{ J/kg K}$ was the constant pressure heat capacity. During forming, with the development of lamellar and molecular orientation, these would change, but for purposes of calculation they were assumed to remain constant. Since the resulting specimen showed only the surface layer that was microstructurally altered during processing, this assumption is reasonable.

The boundary conditions were set using judiciously chosen measured temperatures at various locations in the metal die. It was assumed that each part of the die, being metallic with a high thermal conductivity, had a uniform temperature field (Biot number < 0.1). However, the temperatures of the metal parts of the die increased slowly with time during processing as heat diffused from the heat source at B (Fig. 1). At the slowest forming speeds, the far field temperature approached 80°C . The free end of the specimen was treated as an insulated end. Thermal contact resistance between the metallic parts of the die and the specimen was assumed to be zero and the die and specimen surface in contact were at the same temperature. Experimentally, the die assembly was thermally isolated from the external supports by insulation. Since the strain in the process was limited to a small region near the surface, it was assumed that there was no shape change in the specimen during the processing.

At time equal to zero, the surface nodes of the specimen in contact with the heating plate were assumed to be at the same temperature as the plate, namely, 160°C . The heat flow from the sides of the polymer specimen into the surrounding faces of the die was assumed to be small. The motion through the forming die was simulated by incrementally adjusting the temperatures at the surface nodes of the specimen as it moved from contact with the heated plate to the cooler die walls. As the forming progressed, the amount of polymer (number of nodes) in contact with the hot plate increased, while the number of nodes in contact with the cooler side support plates decreased. The maximum extent of the hot zone was limited by the size of the heated plate ($\sim 50 \text{ mm}$). The mesh used for the calculation had $23 \times 121 \times 11$ nodes.

The calculated two-dimensional temperature distribution on the central longitudinal plane of the specimen is shown in Figure 2 for different times during the processing. The specimen moves from in the $-x$ direction, across the stationary heating plate, with the surface subjected to the strain gradient at the bottom. The leading edge of the heated zone (to the left) corresponds to the point of contact with the lip of the forming die. At this slow forming speed, the shape and extent of the heated zone remains vir-

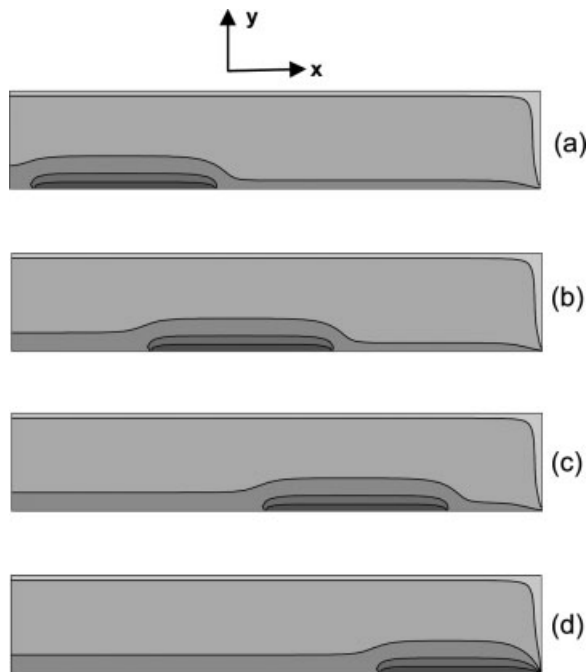


Figure 2 Calculated contours of temperature distribution through the central longitudinal plane of the specimen. The hotter zones are darker. The maximum temperature was 160°C at the bottom surface in contact with the heated plate. The contours are 20°C intervals starting at the minimum plotted temperature (top contour) at 80°C. The forming speed was 0.2 mm/min.

tually constant with respect to the heating plate. The temperature contours shown are for 20°C increments, with the contact surface at 160°C and the outside contour at 80°C. The time for the entire sequence is 40×10^3 s. Although the opposite side of the specimen reaches 80°C, the critical region is the heated zone near the deformation zone in contact with the heater. The extent of this heated zone is limited to the region near the surface where it contacts the heated plate and remains constant over the length of the specimen. The thermal gradient in the deformation zone remains constant along the specimen length.

The temperature fields for a range of different forming speeds (0.2, 0.5, 20, and 50 mm/min) were calculated. At higher processing speeds, the temperature field shape in the longitudinal plane (A) changes shape and extent, as shown in Figure 3. The minimum temperature contour for each processing speed was 80°C, with contours at 20°C intervals. The principal effect at higher speeds is the narrowing of the heat affected zone overall, with higher temperature gradients toward the trailing edge of the zone. This is a result of the low thermal conductivity of the polypropylene. The temperature gradient in the process zone increases with speed.

The effect of speed on the temperature distribution in the transverse plane (B) is shown in Figure 4. The

heated plate is in contact with the bottom surface of the specimen, and the effect of the contact time is clearly seen. At the lowest speeds, the heat flow results in the top surface of the specimen reaching temperatures around 80°C. The sharper temperature gradients at the higher processing speeds are clearly visible.

The increased temperature gradients for high processing speeds in the near surface region of the specimen are shown in greater detail in Figure 5. The arrow indicates higher processing temperatures (0.2, 5, 20, and 100 mm/min). At lower speeds, the gradient is much smaller, and the far field temperature is higher, as the heat has time to diffuse further. The local strain rate depends on the local temperature and the material flow stress at this local temperature. The largest strain rate occurs at the specimen surface, where the temperature is highest ($\sim 160^\circ\text{C}$).

Deformation gradients

Orientation of polypropylene develops with tensile strain at the appropriate temperature (1). The degree of orientation is controlled by the local maximum tensile strain. To measure the strain gradient with minimal disturbance of the temperature field, a small hole was drilled into the specimen, normal to the heated surface of the specimen. The specimen was processed in the normal manner, and the distortion of this line was used to estimate the depth

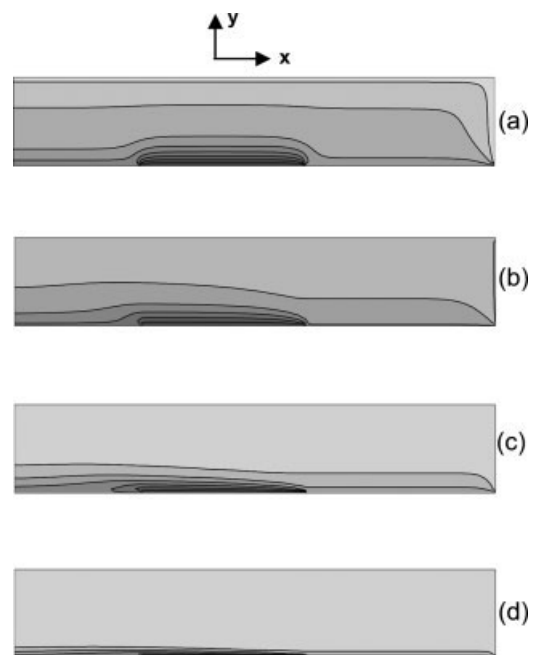


Figure 3 Calculated contours of temperature distribution through the central longitudinal plane of the specimen for different forming speeds: (a) 0.2; (b) 5; (c) 20; and (d) 100 mm/min. The minimum contour starts at 80°C at 20°C intervals.

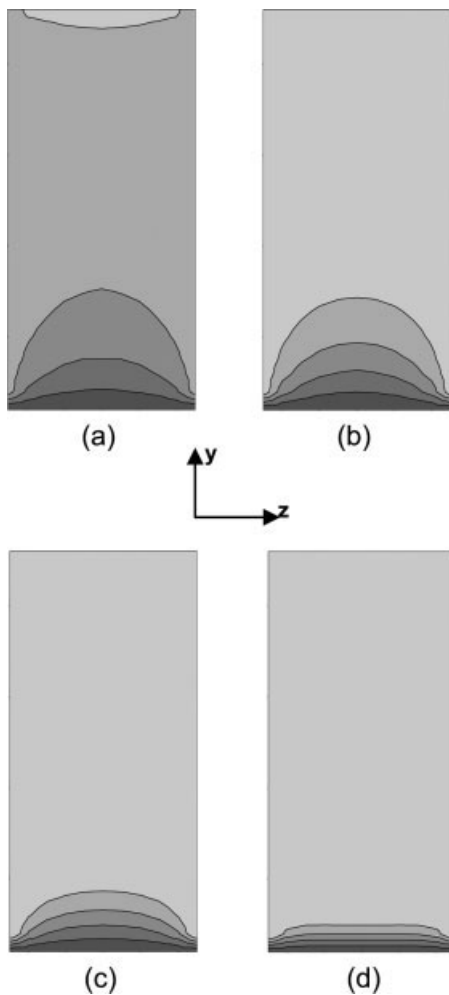


Figure 4 Contours of calculated temperature distribution in the transverse cross-section of the specimen for the different forming speeds shown in Figure 3 [(a) 0.2; (b) 5; (c) 20; and (d) 100 mm/min].

dependence of the processing shear strain. An example for the specimen processed at 0.2 mm/min is shown in Figure 6 (scale bar = 2 mm). The drill hole was initially vertical. It is clear that the thickness of the surface layer in which significant deformation occurs extends to a depth of ~ 2 mm.

The deformation in the near surface region during forming is a simple shear in which the specimen surface is sheared parallel to itself. A fiducial circle transforms to an ellipse with shear strain (inset, Fig. 7). For large strains, Jaeger describes a geometric transformation to calculate the shape of the finite deformation strain ellipse.⁸ From this ellipse, the magnitude and orientation of the principal strain was calculated. The magnitude of the maximum tensile strain was plotted as function of depth (Fig. 7).

The region of the largest tensile strain was confined to the region ~ 2 mm from the surface (Figs. 6 and 7). It was in this near surface region that the greatest change in mechanical properties was ex-

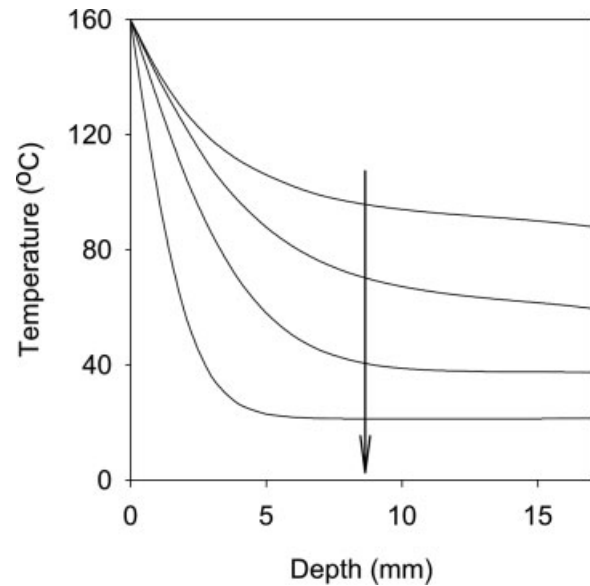


Figure 5 Detailed temperature profiles for increasing forming speeds (arrow). The speeds are 0.2, 0.5, 2, 5, 10, 20, 50, and 100 mm/min.

pected. The two important processing parameters, which control the microstructural gradient, were the processing speed and die temperature. The effect of each these two parameters on local tensile strain is shown in Figure 8, in which the maximum tensile strain was plotted as a function of forming speed and distance from the surface. The three plotted surfaces are for temperatures of 100, 130, and 160°C. The largest tensile strains develop at high temperatures and slow forming rates. These strain gradients produce a microstructural gradient, which controls the mechanical gradient.

It is also evident from Jaeger's analysis that the direction of the resulting maximum tensile strain

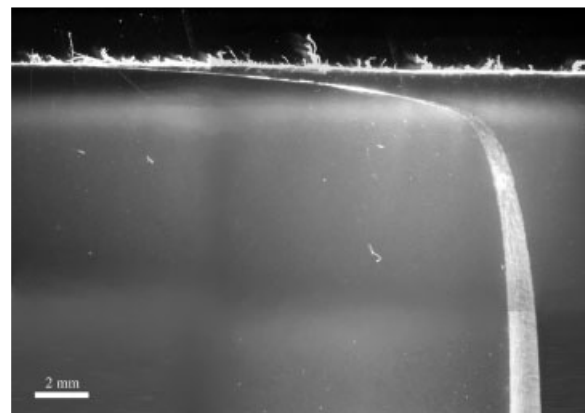


Figure 6 Transmitted light optical micrograph of a cross-section of the near surface region of a processed sample showing the distortion of the initial straight (vertical) fiducial line. The heated surface is at the top. The scale bar is 2 mm. Forming speed 0.2 mm/min.

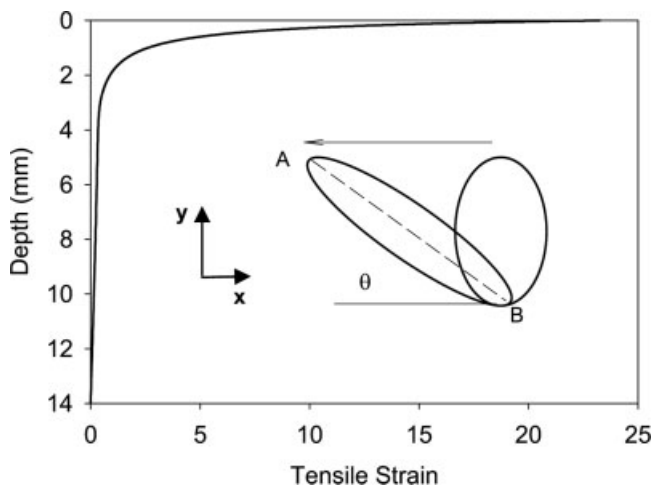


Figure 7 Maximum tensile strain calculated from the measured distortions. Forming speed 0.2 mm/min.

rotates toward the shear plane with increasing applied shear. The increase in shear strain toward the surface results in a rotation of the principal axis of the strain ellipse. Since the molecular orientation follows the direction of maximum tensile strain, at the specimen surface, it is oriented parallel to the surface, but with increasing depth rotates to an angle θ (Fig. 7) with respect to the surface, which depends on the shear strain at that depth. This has been confirmed qualitatively by examining thin sections of the processed specimens in polarized transmitted light. Since the molecular axis lies parallel to the principal strain, measurement of the optical birefringence could be used to define the direction of maximum tensile strain.

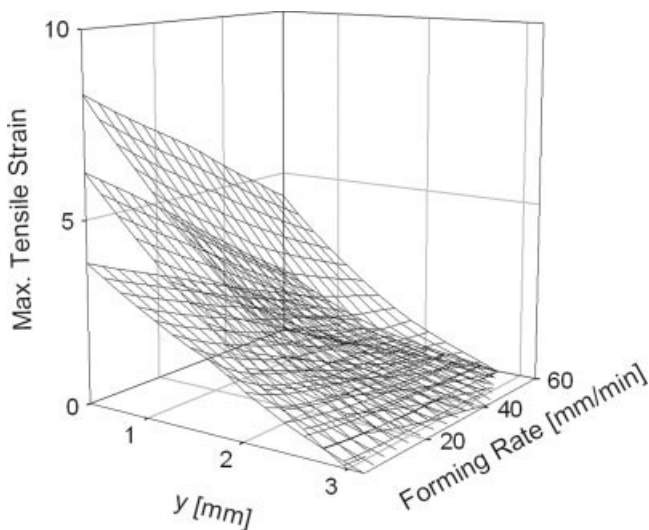


Figure 8 Measured effect of deformation rate and distance from the heated surface on maximum tensile strain. The die temperatures are 100, 130, and 160°C (bottom to top). Forming speed 0.2 mm/min.

Microstructural effects

The material, which developed the largest near surface tensile strains, was examined in greater detail. The strain gradient in the specimen results in a microstructural gradient, which is seen in Figure 9. The processed material was cut into thin sections, parallel to the deformed surface, and examined in the optical microscope in transmitted light under crossed polarizers. The micrographs show that a spherulitic microstructure, typical for unoriented melt-crystallized polypropylene, is found at depths near 2.5 mm from the deformed surface. This is consistent with the depth at which the tensile strain becomes negligible (Fig. 7) is small. In regions approaching the top surface, the spherulites elongate with higher aspect ratios approaching the surface within this layer thickness. At large tensile strains,

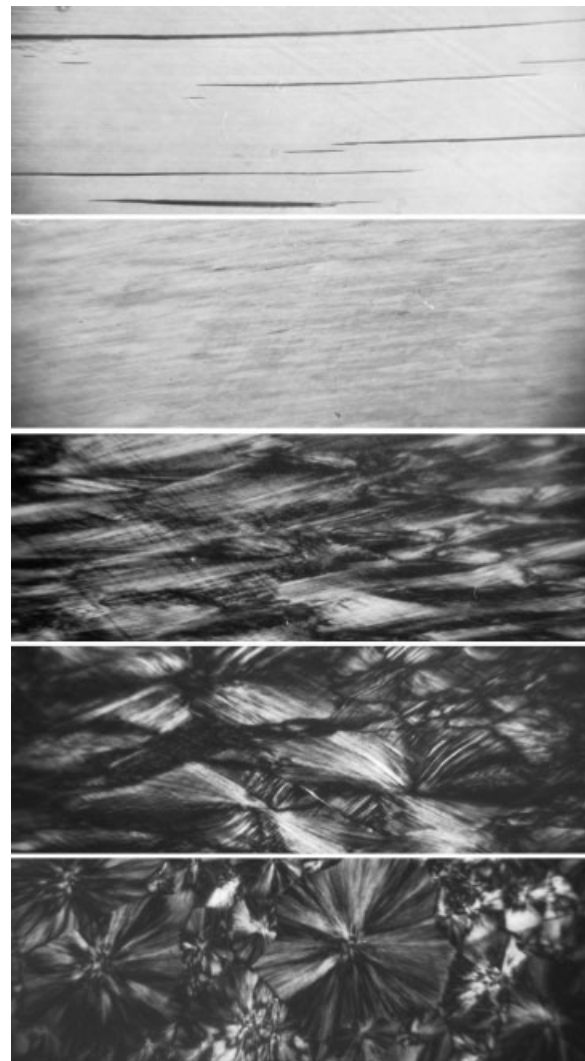


Figure 9 Transmitted light optical micrographs (crossed polarizers) of cross-sections from depths 0.8, 1.5, 1.9, 2.1, and 2.5 mm from the heated surface (which is at the top). Forming speed 0.2 mm/min.

the spherulites disappear as the microstructure becomes disrupted. The overall optical birefringence of the oriented molecules is much stronger closer to the surface, consistent with improved degree of orientation. In the region closest to the surface, microcracking parallel to the orientation direction appears, as the large tensile strains begin to form the elongated voids characteristic of hot drawn polypropylene (1).

The DSC scans comparing surface to core material after processing are shown in Figure 10. These are heating scans, with the peaks representing the melting endotherms. An unoriented material (A) shows a single peak typical of spherulitic polypropylene. The surface region of the processed sample shows an endotherm with two peaks at 152 and 162°C (B). These indicate the presence of two distinct populations of lamellae, the first a metastable crystallite and the second the equilibrium structure.⁹ This can be explained as follows.

The thermomechanical process in the near surface region involves a large plastic strain at elevated temperature, similar to a process of hot drawing in which the original lamellar and spherulitic structure is destroyed (by interlamellar and intralamellar deformation mechanisms), and subsequently recrystallized into the familiar oriented structure. The highly deformed surface region has the same monoclinic crystal structure as the undeformed core material (Fig. 11). The surface region shows a moderate degree of orientation, similar to that seen in hot drawn material (Fig. 12). As expected, the strong (110) peak lies in a plane normal to the direction of

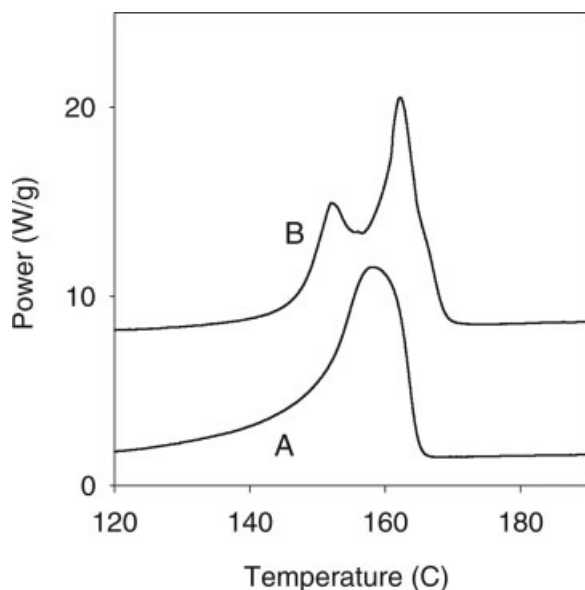


Figure 10 Differential scanning calorimetry heating scans for (A) core material (unoriented) and (B) surface material (oriented). Forming speed 0.2 mm/min.

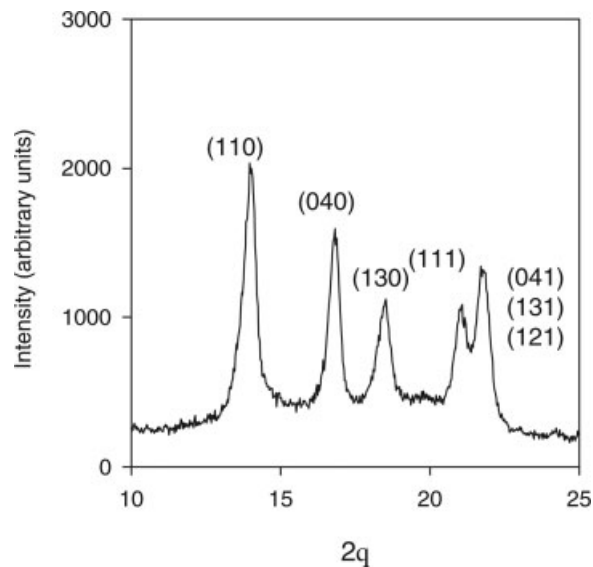


Figure 11 Indexed X-ray diffractometer scan of near surface material. Forming speed 0.2 mm/min.

maximum tensile strain, indicating the lamellae normal lie parallel to the maximum tensile strain (i.e., the molecular axis is parallel to the principal strain axis). The X-ray specimens are ~ 1 mm thick, and so the diffraction pattern in Figure 12 represents the average orientation over that depth dimension.

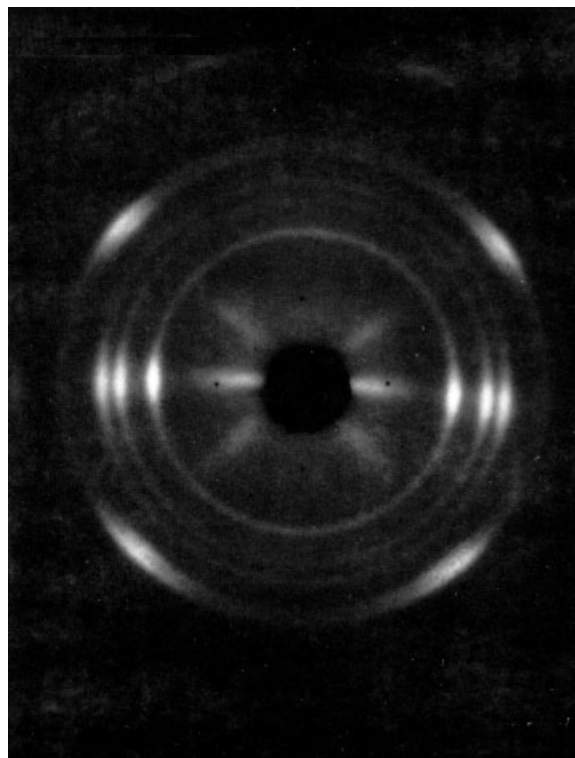


Figure 12 Transmission X-ray diffraction pattern of near surface material in formed sample (the orientation direction is vertical) (Ni-filtered $\text{Cu K}\alpha$). Forming speed 0.2 mm/min.

Hot-deformed polypropylene is expected to have a distribution of lamellar sizes and defect densities, which depend on the local temperature and strain during deformation.^{10,11} More recently, a similar microstructural evolution, which develops at large plastic strains has been reported for hot-deformed syndiotactic styrene/*p*-methyl styrene copolymer.¹²

In general, the relative stability of microstructures, which evolve on hot drawing, depends on the temperature and strain rates imposed during deformation. Recrystallized structures produced at the higher deformation temperatures are more stable, while at lower temperatures and higher strain rates, the structures tend to be less stable, with significant internal stresses from unrelaxed amorphous material and high defect content in crystals. The reported equilibrium melting temperature for crystalline polypropylene is 186.1°C,¹³ which suggests that the original and deformed polypropylene in the present study are "nonequilibrium," with the higher melting temperature endotherm representing a relatively stable form of the crystal. For the present experiments, the finite thickness (0.2–0.3 mm) DSC samples contain a mixture of microstructures since there is a sharp gradient in temperatures, strains, and strain rates in the deformed specimen.

The multiple melting peaks seen in Figure 9 can be explained in terms of different lamellar thicknesses.¹³ The peak temperatures are consistent with long periods in the range 10–17 nm, which is in the range reported for hot-drawn polypropylene.¹ The smaller lamellae melt at the lower temperatures and can recrystallize to form larger crystals, which subsequently melt at the higher temperatures during the DSC heating.

A more detailed explanation for the multiple melting peaks in drawn polypropylene has been suggested by Yan et al.¹⁴ The low temperature DSC peak was associated with constrained crystallization during drawing. The second peak temperature depended on the draw ratio and hence was different from the spherulitic melting peak temperature of the undeformed material. It was suggested that the two peaks represent two crystal thicknesses, found outside, and within the microfibrils, which are produced during large strain tensile deformation in polypropylene. The first crystal was thought to be a quasi-amorphous crystal, presumably with high defect content similar to that described by Ward and coworkers.¹⁵ The second peak was interpreted to arise from the melting of standard folded chain lamellar crystals. Yan et al.¹⁴ suggested that upon melting in the DSC, the metastable material melts at the lower peak temperature and partially recrystallizes to form the lamellar morphology with a higher melting temperature. The process of recrystallization has also been suggested by others as a source of double-melting peaks.^{16,17}

Gradient of mechanical properties

The in-plane stiffening of the surface layer can be seen in Figure 13, in which the measured temperature-dependent storage modulus (parallel to *z*, the forming direction) is shown. The material (A) from the near surface region of the processed sample is much stiffer than the core, unoriented material (B). The oriented material was cut from a thin slice at the surface (thickness = 1.7 mm) of the processed specimen, in a sample formed at a speed of the 0.2 mm/min.

The anomalous increase in modulus approaching 150°C may be due to the recrystallization of the metastable "quasi-crystals" proposed by Yan et al.,¹⁴ as

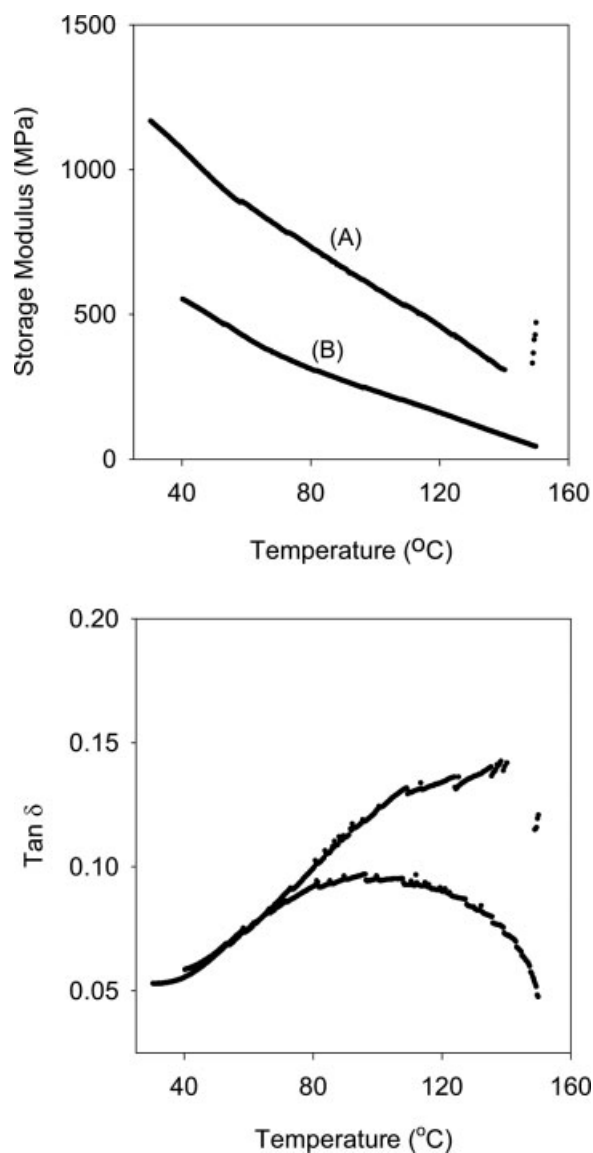


Figure 13 Dynamic mechanical thermal analysis of (A) surface and (B) core. The top figure is the storage modulus and the bottom is the loss tangent. Forming speed 0.2 mm/min.

the material is heated through this temperature range. The average modulus of the crystalline fraction can increase as a result of recrystallization in the DMTA. Heating replaces crystals with high defect density with those, which are more "perfect." Crystals with high defect density have a lower modulus than more "perfect" crystals. The loss tangent for the unoriented core shows the characteristic broad maximum near 100°C, which is the expected β relaxation for polypropylene. However, the oriented material shows a continuous rise in loss with increasing temperature, suggesting the shift of the broad β peak to higher temperatures in this oriented surface material. The crystallization near 150°C appears as the sudden drop in loss near the end of the test.

An alternative explanation for the anomalous rise in modulus at high temperatures may be from an increase in the entropic retractive stress parallel to the orientation direction, which results from the shrinkage of the specimen. However, there was no experimental evidence for any significant distortion of the specimen during the heating for the DMTA.

Microindentation

The use of displacement-controlled microindentation to measure local mechanical properties has been described earlier.^{2,3,18-21} Unlike standard hardness tests, in which a prescribed load is applied to a tapered tip, these tests control the tip position in displacement control. The deep penetration tests involve the constant velocity indentation to depths of the order (and greater) than the tip diameter. In homogeneous isotropic polymers, an analysis of the stress and strain fields under the flat punch microindenter shows that the stress field is largely restricted to a region ~ 1 tip diameter in front of the tip. The spatial resolution in the transverse plane is slightly larger than the tip diameter. By using different tip diameters, the spatial resolution of the measurement can be adjusted.

The phenomenology of inelastic deformation in front of the moving tip has been reported for unoriented polymers.² Recent work on deep penetration microindentation of oriented polypropylene has studied the micromechanics under the tip for penetration parallel to the orientation direction.²¹ It was noted that indentation perpendicular to the orientation direction was considerably "harder" than tests parallel to the molecular axis. The modulus, however, was notably smaller in the transverse direction. A qualitative understanding of the mechanical behavior under the indenter tip is as follows.

The sharp discontinuity at the outer edge of the tip face generates a large stress in the polymer. Yield initiates in these small local volumes. With increas-

ing penetration, the plastic zone increases in size, moving ahead of the tip. The plastically deforming material is pushed aside as the indenter tip moves down into the material. The critical indentation stress depends on the elastic and plastic properties of the material, which resists the movement of material to the side of the indenter as it moves. Ignoring the work-hardening characteristics of the material, the indenter stress is related to the yield stress of the material, which, in turn, is represented by the constraint factor.¹⁸⁻²⁰ For anisotropic polymers, the elastic and plastic anisotropy strongly affect the deformation mechanisms in the material. The load-displacement output from the test can be normalized for specific microstructures, and the tensile yield stress for the material estimated.²

For a continuum solid, with no microstructural inhomogeneities, the mechanics of indentation scale with the tip diameter, and results from different tip diameters can be normalized with respect to the tip diameter. The flat cylindrical microindenter therefore samples a volume of material restricted to the region ~ 1 diameter around the face of the moving tip. The plastic zone develops as the indenter moves into the material, until at a depth of less than $\frac{1}{2}$ diameter, a steady-state deformation zone has developed. The increasing punch stress at small depths of indentation is linear with depth, the observed hardening due to an increasing plastic volume. The steady state is indicated by the smooth decrease in slope of the stress-displacement curve.

Microindentation stress-displacement curves are shown in Figure 14. The tests were performed at different depths from the processed surface. In this

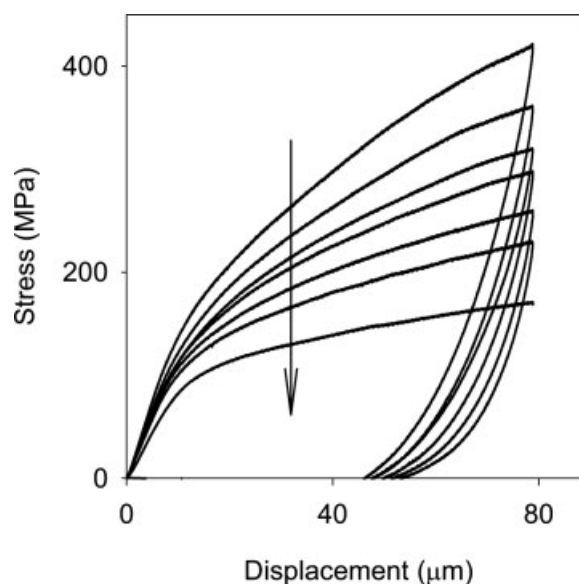


Figure 14 Deep penetration microindentation tests for increasing depths (arrow) from the formed surface (0.6, 1.2, 1.6, 1.8, 2.0, and 2.2 mm). Forming speed 0.2 mm/min.

TABLE I
Depth Dependent Yield Stress

Distance from Surface (mm)	Strain	Yield stress (MPa) $P_m = 2.6 \sigma_y$
0.63	4.70	51.1
1.20	2.03	49.3
1.57	1.32	48.4
1.77	1.08	47.9
2.00	0.89	45.9
2.23	0.73	41.5

way, the penetration curves could be analyzed following the earlier normalization procedures. Tabor suggested that the large displacement linear portion of the curve could be extrapolated back to the zero displacement axis to obtain the intercept with the stress axis (9). This stress is proportional to the tensile yield stress of the material. This was confirmed in earlier work on unoriented polyethylene.² In the present case, a Tabor factor of 2.6 was estimated. The tensile yield stress calculated from the microindentation tests of Figure 14 are shown in Table I. A clear strengthening is observed in the material closer to the surface.

The higher degree of orientation and resulting higher measured hardness is accompanied by an increase in extent of cracking around the residual indentation after the indenter is removed (Fig. 15). The images are taken in from reflected light from different depths. Each image represents a residual indentation from a deep penetration test run by successively polishing back the surface to the depths

indicated before running the test. The surfaces were coated with thin a reflective AuPd layer (~ 15 nm) deposited after testing by vacuum evaporation.

Cracking closer to the surface reveals progressively larger residual cracks of a similar nature to those shown here. The cracking is consistent with the increased degree of orientation closer to the surface. The practical result is that although the penetration resistance at the surface is increased, the extent and amount of longitudinal cracking is also increased. The cracking, however, does not affect the resilience of the surface to normal penetration, as indicated by the large displacements recovered in the microindentation curves.

For the specimen formed at 0.2 mm/min, the changes in mechanical response of the material therefore appear to occur in the surface layer to a depth of ~ 2 mm. The depths for other forming speeds at which the forming temperature is the same can be estimated from Figure 5. These are plotted in Figure 16 as a function of forming speed. This depth represents the thickness of the near surface region within which the material is expected to be substantially deformed during processing. The thickness of the processed near surface layer saturates at about 0.5 mm and further increases in forming speed produce negligible changes. The evolution of microstructure at a particular depth, of course, depends additionally on the local strain rate and state of stress, which are not known. The increasing localization of the strain at higher forming speeds, however, is consistent with the observation of increased longi-

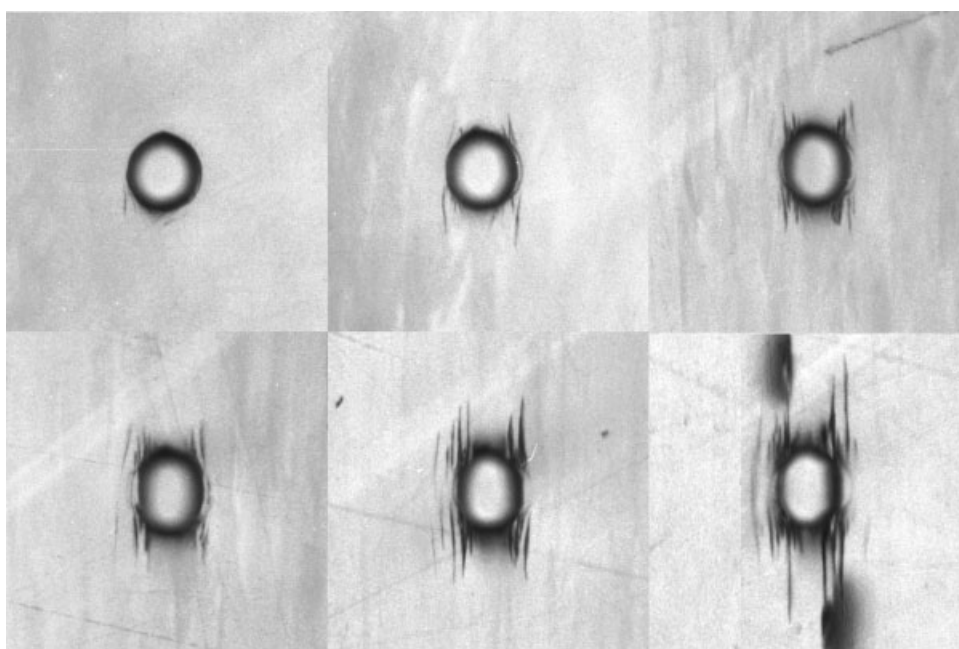


Figure 15 Cracking surrounding the residual indentations in the surface (80 μ m diameter) as a function of depth (2.2, 2.0, 1.8, 1.6, 1.4, and 1.2 mm). The cracks are parallel to the orientation direction. Forming speed 0.2 mm/min.

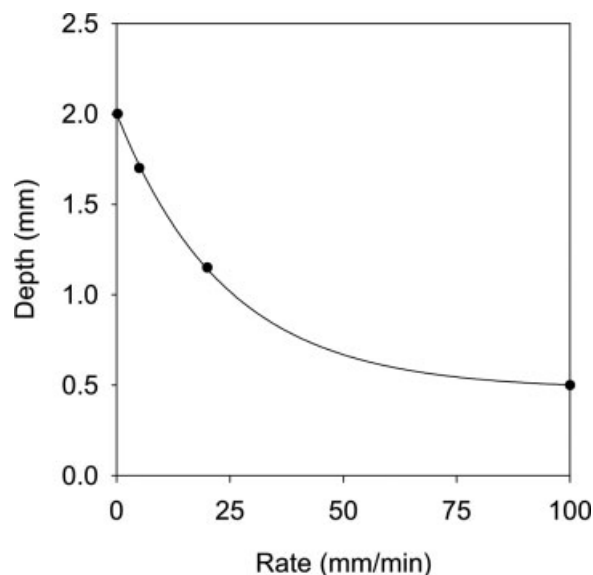


Figure 16 Thickness of the near surface deformation zone as a function of forming speed. Estimated from Figure 5.

tudinal cracking at high speeds: resulting from the larger internal stresses for high strain gradients.

CONCLUSIONS

The deformation of the near surface region in polypropylene can be controlled to some extent by adjusting the temperature distribution, which affects the strain gradient. The microstructural variation across this thin zone has been examined and correlated with the measured gradient in mechanical properties.

The assistance of Mr. Bert Verhagen in completing the experimental work is gratefully acknowledged.

References

1. Shinozaki, D. M.; Groves, G. W. *J Mater Sci* 1973, 8, 119.
2. Lu, Y.; Shinozaki, D. M. *Mater Sci Eng A* 1998, 249, 134.
3. Lu, Y.; Shinozaki, D. M. *Polym Eng Sci* 1997, 37, 1815.
4. Capaccio, G.; Gibson, A. G.; Ward, I. M. In *Ultra-High Modulus Polymers*; Ciferri, A.; Ward, I. M., Eds.; Applied Science Publishers: London, 1979; Chapter 1.
5. Merrygold, E.; Osman, F. H. *J Mater Process Technol* 1998, 80, 179.
6. Yamauchi, T. *J Appl Polym Sci* 2006, 100, 2895.
7. Springer, H.; Schenk, W.; Hinrichsen, G. *Colloid Polym Sci* 1983, 261, 9.
8. Jaeger, J. C. *Elasticity Fracture and Flow with Engineering and Geological Applications*; Wiley: New York, 1969.
9. Wunderlich, B. *Thermal Analysis*; Academic Press: Boston, 1990.
10. Balta-Callega, F. J.; Peterlin, A. *J Mater Sci* 1969, 4, 722.
11. Stern, C.; Frick, A.; Weickert, G. *J Appl Polym Sci* 2007, 103, 519.
12. Yan, R. J.; Aiji, A. J.; Shinozaki, D. M. *Polym Eng Sci* 2001, 41, 1674.
13. Mezghni, K.; Campbell, R. A.; Phillips, P. J. *Macromolecules* 1994, 27, 997.
14. Yan, R. J.; Jiang, B. *J Polym Sci Part B: Polym Phys* 1993, 31, 1089.
15. Tariya, A. K.; Unwin, A. P.; Ward, I. M. *J Polym Sci Phys* 1988, 26, 817.
16. Kamide, K.; Yamaguchi, K. *Macromol Chem* 162, 205 1972.
17. De Rosa, C.; Gurra, G.; Petracone, V.; Tuzi, A. *Polym Commun* 1987, 28, 143.
18. Tabor, D. *Rev Phys Technol* 1970, 1, 145.
19. Tabor D. In *Microindentation Techniques in Materials Science and Engineering*; Blau, P. J.; Lawn, B. R., Eds.; American Society for Testing and Materials: Philadelphia, 1986, pp 129–159.
20. Tabor, D. *Philos Mag A* 1996, 74, 1207.
21. Lo, J. C. W.; Lu, Y. C.; Shinozaki, D. M. *Mater Sci Eng A* 2005, 409, 76.